



Optimization and synthesis of etoricoxib-loaded low molecular weight chitosan nanoparticles

Aulia Rhamdani Arfan¹  Auliya Ilmiawati¹  Purwantiningsih Sugita^{1*} 

Department of Chemistry, Faculty of Mathematics and Natural Sciences, University – Bogor (IPB), 16680, Indonesia, Ásia.
E-mail: purwantiningsih@apps.ipb.ac.id. *Corresponding author.

ABSTRACT: This study reports the optimization of the preparation of etoricoxib (ETX)-loaded low molecular weight of chitosan (LMWC) nanoparticles (ETX-LMWC-NPs) by ionic gelation method with sodium tripolyphosphate (TPP) as cross-linking agent. The independent variables (LMWC/TPP mass ratio, LMWC, and poloxamer 188 concentration) were formulated and optimized using response surface methodology (RSM) Box-Behnken design (BBD) with three levels for each factor. Size of particles, polydispersity index (PDI), and encapsulation efficiency was investigated as the dependent variable. ETX-LMWC-NPs were characterized by particle size analyzer, scanning electron microscope, UV-Vis spectrophotometry, and Fourier transforms infrared spectroscopy. The ETX-LMWC-NPs have an average particle size of 259.91 nm, a PDI of 0.041, and encapsulation efficiency of 51.25%. ETX-LMWC-NPs are spherical and have a spectrum at wavenumber 1656 cm^{-1} and 718 cm^{-1} , respectively, indicating the presence of C=N and C-Cl originating from the ETX compound. The ETX release profile at pH 1.2 and 6.8 mediums approach the Korsmeyer-Peppas model. ETX released pH 1.2 did not differ significantly from free ETX with a maximum 10-12% release. ETX release at pH 6.8 had a maximum release of 21% and showed a 19% increase in dissolution rate than free ETX. The ETX-LMWC-CSNPs prepared by optimum formula (2.65 % LMWC, 5.5 LMWC/TPP mass ratio, and 1 mg/mL) showed stable monodispersity nanoparticles and easily soluble in water.

Key words: chitosan, ntoricoxib, nanoparticle, poloxamer 188.

Otimização e síntese de nanopartículas de quitosana de baixo peso molecular carregadas com etoricoxib

RESUMO: Este experimento relata a otimização da preparação de nanopartículas de quitosana de baixo peso molecular (LMWC) (ETX-LMWC-NPs) carregadas com etoricoxibe (ETX) pelo método de gelificação iônica com tripolifosfato de sódio (TPP) como agente de reticulação. As variáveis independentes (razão de massa LMWC / TPP, LMWC e concentração de poloxamer 188) foram formuladas e otimizadas usando metodologia de superfície de resposta (RSM) projeto Box-Behnken (BBD) com três níveis para cada fator. Tamanho das partículas, índice de polidispersidade (PDI) e eficiência de encapsulação foram investigados como a variável dependente. ETX-LMWC-NPs foram caracterizados por analisador de tamanho de partícula, microscópio eletrônico de varredura, espectrofotometria UV-Vis e espectroscopia de infravermelho com transformada de Fourier. Os ETX-LMWC-NPs têm um tamanho médio de partícula de 259,91 nm, um PDI de 0,041 e eficiência de encapsulação de 51,25%. ETX-LMWC-NPs são esféricos e apresentam um espectro no número de onda 1656 cm^{-1} e 718 cm^{-1} , respectivamente, indicando a presença de C = N e C-Cl originários do composto ETX. O perfil de liberação de ETX em meios de pH 1,2 e 6,8 se aproxima do modelo Korsmeyer-Peppas. O ETX liberado em pH 1,2 não diferiu significativamente do ETX livre com uma liberação máxima de 10-12%. A liberação de ETX em pH 6,8 teve uma liberação máxima de 21% e mostrou um aumento de 19% na taxa de dissolução do que o ETX livre. Os ETX-LMWC-CSNPs preparados pela fórmula ótima (2,65% LMWC, 5,5 LMWC / razão de massa TPP e 1 mg / mL) mostraram nanopartículas de monodispersidade estáveis e facilmente solúveis em água.

Palavras-chave: etoricoxib, nanopartícula, poloxamer 188, quitosana.

INTRODUCTION

Etoricoxib (ETX), or chemically known as 5-chloro-6'-methyl-3-[4-methylsulfonyl phenyl]-2, 3'-bipyridine, is one of the selective non-steroidal antiinflammation drugs (NSAIDs) (TAKEMOTO et al., 2008). ETX is used to relieve the pain in patients with gouty arthritis, rheumatoid arthritis,

ankylosing spondylitis, and osteoarthritis (CROOM & SIDDIQUE, 2009; TAKEMOTO et al., 2008). ETX has been reported as a potent drug over other traditional NSAIDs because of its high selectivity to inhibit cyclooxygenase-2 or COX 2 (an enzyme responsible for inflammation and pain in organs) and has gastrointestinal tolerance (FENG et al., 2018). Despite ETX advantages, the use of ETX is not

approved by the US Food and Drug Administration (FDA) (ESCUDERO-CONTRERAS et al., 2007), as well as the Brazilian Agency of Sanitary Surveillance (ANVISA), which restricted the use of ETX (Arcoxia) with dose 120 mg (FRACON et al., 2010). Side effects of ETX were the main reason for the restriction of etoricoxib in the US and Brazil, such as its potent COX-2 inhibition could induce blood clotting (ESCUDERO-CONTRERAS et al., 2007), narrowing blood vessels, high blood pressure (BIRMINGHAM & BUVANENDRAN, 2013), and cardiovascular disease (SASICH et al., 2008). Besides, ETX has shown poor aqueous solubility, poor dissolution, low absorption rate (DAS et al., 2011; PATEL et al., 2007), and high protein binding ability (TAKEMOTO et al., 2008). Those ETX properties impact the diminishing volume of distribution difficulty passing cell membranes and low bioavailability in the inflammation area (WANAT, 2020). So, it requires a higher dose to treat the pain in the patient. AGRAWAL et al. (2001) reported that ETX main bioavailability in plasma increased linearly with the increase of ETX dose and has 101% bioavailability at 120 mg of ETX (TAKEMOTO et al., 2008). However, as mentioned above, 120 mg ETX dose is restricted to consume in Brazil by ANVISA and only small doses such as 60 mg and 90 mg that allowed to consume with safety warning related to its side effects (FRACON et al., 2010).

To overcome these drawbacks, we proposed delivering ETX by loading or encapsulating ETX inside the material with a diameter particle ranging from 1-1000 nm or referred to as nanoencapsulation (KITA & DITTRICH, 2011). Nanoencapsulation offers several improvements of drug properties such as drug solubility, bioavailability, and enhanced therapeutic activity of drug with the minimum side effect (JONG & BORM, 2008). Also, nano-size formed by nanoencapsulation showed better mobility (SINGH & LILLARD JR., 2009) and higher ability to enter the cell by passive uptake than the large particles (JONG & BORM, 2008; SHANG et al., 2014).

Chitosan is one of the abundant biopolymers that has been applied and developed as a drug delivery material for more than two decades (NASKAR et al., 2019). Its environmentally friendly, biodegradability, biocompatibility, and mucoadhesive properties made chitosan a promising delivery agent for drugs (LI et al., 2018). Previous studies have been reported ETX delivery attempts using modified or hybrid chitosan with different shapes and properties, such as cubic nanoparticles formed by chitosan-Kheri gum polyelectrolyte complex (MALVIYA et al., 2020), aldehyde chitosan, and chitosan HPMC

(hydroxypropyl methylcellulose) film aldehyde chitosan hydroxypropyl-methyl cellulose (WAHID et al., 2008), and chitosan-sodium alginate microbeads (KAUR & PALIWAL, 2019). However, those studies required a high cost and used high molecular weight chitosan (HMWC), which has higher hemostatic activity and elevates the blood coagulation effect of ETX. HMWC molecules have a higher blood coagulant effect (HU et al., 2018) than LMWC that cannot form strong blood coagulants (INAMDAR & MOURYA, 2014). According to that, low molecular weight chitosan (LMWC) is required as encapsulating material of ETX.

Low molecular weight chitosan (LMWC) is one of the chitosan developing results produced by HMWC degradation. Unlike HMWC, LMWC indicated more advanced properties such as less toxicity, high solubility in water (FAN et al., 2012; LEE et al., 2001), and unable to establish firm blood coagulum (HU et al., 2018). Based on these advantages, LMWC is chosen as a suitable material to deliver ETX. Furthermore, LMWC could form stable monodisperse (PDI < 0.05) (DANAEI et al., 2018) chitosan nanoparticles with narrow size by the ionic gelation method (FAN et al., 2012).

The objective of this research was to prepare ETX loaded in LMWC nanoparticles by the ionic gelation method. Synthesis based on optimizing the formulation variables using the response surface methodology a three-level and a three-factor of Box Behnken design (BBD) as a template. ETX-LMWC nanoparticles are characterized by particle size, polydispersity index (PDI), encapsulation efficiency, shape, functional groups, and in vitro release behaviour.

MATERIALS AND METHODS

Etoricoxib (ETX) in this study was given by PT Dexa Medica, Indonesia. The low molecular weight of chitosan (LMWC) (12576 Da) and poloxamer 188 were purchased from Xi'an Sgonek Biological Technology Co. Ltd, China. Sodium tripolyphosphate (TPP) was purchased from Merck Chemicals Co. All other reagents and solvents were of analytical grade.

Preparation of ETX-LMWC-NPs

The ETX-LMWC-NPs were prepared by a modified ionic gelation method reported in the previous study (SUGITA et al., 2015). Low molecular weight of chitosan (LMWC) 2.5 g was dissolved in acetic acid 2% (v/v) and left under stirred for 10 minutes. TPP 2.5 g was dissolved separately in 100 mL of deionized

water. LMWC solution and TPP solution were filtered before use. 20 mL poloxamer 188 in deionized water, as a stabilizer, was dripped into LMWC solution under stirring. Then 40 mL ETX 0.2 mg/mL in ethanol was dropped into LMWC solution under stirring, followed by TPP 2.5 % (w/v) added drop by drop into the mixture under stirring. Subsequently, the solution was stirred for another 10 minutes to form chitosan nanoparticle suspension. The particle size and its distribution of ETX-LMWC-NP were determined using a VASCO particle size analyzer in a single measurement for each sample. The suspension nanoparticles were then dried by spray dryer mini Buchi 190, continued by morphology characterization by scanning electron microscopy (SEM) Hitachi SU-3500 and functional groups using Fourier transforms infrared spectroscopy (FTIR) Perkin Elmer Spectrum One.

Evaluation of influence LMWC/TPP mass ratio towards ETX-LMWC-NPs

Evaluation was carried out on LMWC/TPP mass ratios: 2.5; 3.5; 4.5; 5.5, and; 6.5 (75, 105, 135, 165 and 195 mL of LMWC 2.5% respectively) as independent variable, while 30 mL TPP 2.5%, 1 mg/mL poloxamer 188 and 0.2 mg/mL ETX as control variables.

Evaluation of influence LMWC concentration towards ETX-LMWC-NPs

Evaluation was carried out on 135 mL 2.5%, 3.0% and 3.5% LMWC as independent variable while 30 mL TPP 2.5%, 1 mg/mL poloxamer 188 and 0.2 mg/mL ETX as control variables.

Evaluation of influence poloxamer 188 concentration towards ETX-LMWC-NPs

Evaluation was carried out on poloxamer 188 with concentration 0 mg/mL; 1 mg/mL; 1.5 mg/mL and 2 mg/mL as independent variable, while 135 mL LMWC 2.5%, 30 mL TPP 2.5% and 0.2 mg/mL ETX as control variables.

Optimization the formula of synthesis ETX-LMWC-NPs

In order to form ETX-LMWC-NPs with stable monodisperse nanoparticles (PDI < 0.05), mean particle in nano-size (1-1000 nm) and encapsulation efficiency close to 100%. The optimization formula was performed using response surface methodology (RSM). In this study, Box-Behnken design was chosen as a template for RSM with three levels three factors, formulated and analyzed using software Design Expert 13. The design comprised 15 experimental

that included 12-factor points and three replications at the center point.

Determination of encapsulation efficiency

Nanoparticles suspension were dried by spray dryer at inner temperature 80-100 °C to get nanoparticle powder. Nanoparticles powder (25 mg) was extracted in 50 mL phosphate saline buffer (PBS) pH 7.4, and then the mixture was shaken by linear shaker 240 strokes/minute for 24 hours at 37 °C. After that, the nanoparticle solution was filtered by a nylon syringe filter 0.22 µm to remove nanoparticles pellets. Supernatant that was collected then measured by Thermo Scientific Genesys 10S Ultraviolet-Visible at 234 nm. The efficiency encapsulation (EE) was calculated using equation (1). Efficiency encapsulation determination of 15 formulas designed by Box-Behnken optimum formulas were carried out in triplicate each sample.

$$EE(\%) = \frac{(x \text{ mg/mL}) \times V \times \frac{a}{b}}{m} \times 100 \% \quad (1)$$

Note: x = concentration of ETX

V = extraction volume

a = amount of nanoparticles powder that extracted in PBS

b = total amount of nanoparticles powder

m = total mass of etoricoxib

In-vitro release study

In vitro ETX release from ETX-LMWC-NPs was evaluated using the dialysis sac method in medium, time, and temperature adapted to gastric acid (buffer KCl-HCl pH 1.2 for 3 hours) and intestinal liquid (PBS pH 6.8 for 6 hours) (HWANG et al., 2008). Dialysis tube semi-permeable cellulose membrane with molecular weight cutoff 14 kDa was soaked in deionized water for 12 hours before use. ETX-LMWC-NPs powder (500 mg) was dispersed in 5 mL of buffer solution, then transferred to the dialysis tube as donor compartment, sealed with a rope, and suspended in 500 mL buffer solution in the receiver compartment. ETX release in vitro was performed in a water bath linear shaker with 200 strokes/minute at 37 °C. Samples from the receiver compartment were collected 15 mL every 15 minutes and replaced with the new buffer solution to maintain total volume. The amount of released ETX from nanoparticles was determined using Thermo Scientific Genesys 10S Ultraviolet-Visible at 234 nm. The experiments were done in triplicates and compared with unencapsulated ETX (pure etoricoxib). The obtained release data were then fitted with appropriate release kinetic models.

RESULTS AND DISCUSSION

Influence of LMWC/TPP mass ratio to character of ETX-LMWC-NPs

Particle size and its distribution were reported to have an essential effect on the drug delivery system (SHANG et al., 2014). According to that statement, we studied LMWC and TPP concentrations ratio, which have a vital role in controlling particle size and distribution (KOUKARAS et al., 2012). Table 1 shows the LMWC/TPP mass ratio's influence on particle size, polydispersity index, and encapsulation efficiency by adding 30 mL of TPP to a few different LMWC volumes (75 mL to 195 mL). The particle size decreased from 287 nm to 148.13 nm linearly with ratio augmentation till 5.5 and increased to 183.10 nm when 195 mL of LMWC was added (mass ratio 6.5). This phenomenon was also reported in the previous studies (ANTONIOU et al., 2015; FAN et al., 2012; KOUKARAS et al., 2012) with lower chitosan and TPP concentrations.

The large particle size formed with a ratio of 2.5 was caused by the amount of TPP ($P_3O_{10}^{5-}$) being more than the other LMWC/TPP mass ratios. The excess TPP anions in low concentrations of chitosan facilitate particle bridging and aggregation of particles (HUANG et al., 2015). Aggregation led to a variety of particle sizes, and wide particle size distribution resulted in a high value of PDI (0.100). Moreover, a high concentration of TPP has strong cross-linking interaction with chitosan molecules, high cross-link density, and formed compact nanoparticles. Mass ratio enhancement or reduced TPP concentration shown decreasing mean particle size and lower PDI value.

Conversely, the LMWC/TPP mass ratio of 6.5 produced nanoparticles with a larger size than the ratio of 4.5 and 5.5 due to the insufficient number

of TPP anions to interact with the NH_3^+ cation in the LMWC chain. This phenomenon causes weaker and lower cross-linking interaction the $P_3O_{10}^{5-}-NH_3^+$ than the other LMWC/TPP ratios, and limited TPP adsorption surface of nanoparticles and facilitating inter-particle interactions and aggregation (HUANG et al., 2015) and resulting in wide particle size distribution or high PDI value (0.093).

The encapsulation efficiency of ETX in LMWC-NPs based on mass ration LMWC/TPP shows fluctuated results caused by nanoparticles' compact and swollen character. Swollen nanoparticles formed by 6.5 mass ratios have higher efficiency than nanoparticles from other ratios. The swollen nanoparticles have more free space between polymer chains to load more drugs (BOGUSZ et al., 2019). Compared with a compact nanoparticle with little space between polymer chains to load drugs, this is proven by encapsulation efficiency of nanoparticles formed by 2.5:1 only has 39%. Based on the size of the nanoparticles and their PDI, the nanoparticles formed from the mass ratio of LMWC/TPP of 4.5 (135 mL LMWC and 30 mL TPP) are the most stable. However, the formula has very low encapsulation efficiency. Therefore, a further formula optimization study was conducted using the response surface methodology at a ratio of 3.5, 4.5 and, 5.5.

Influence of LMWC concentration on character of ETX-LMWC-NPs

The results of the evaluation of the LMWC concentration are shown in table 2 — the table shows linear enlargement in mean particle size with increasing LMWC concentration. Particle size enlargement could be created by interactions between intra- and inter molecules of LMWC. Chitosan has semi-crystalline properties formed in powder due to hydrogen bonds, hydrophobic interactions, and van

Table 1 - Influence of LMWC/TPP mass ratio to character of ETX-LMWC-NPs.

LMWC/TPP mass ratio	Mean particle size (nm)	PDI	Encapsulation efficiency (%)
2.5	287.00	0.100	39.0924
3.5	229.74	0.050	49.8595
4.5	178.86	0.009	35.1007
5.5	148.13	0.041	44.2786
6.5	183.10	0.093	51.1720

Table 2 - Influence of LMWC concentration to character of ETX-LMWC-NPs.

LMWC (%)	Mean particle size (nm)	PDI	Encapsulation efficiency (%)
2.5	178.86	0.0090	35.1007
3.0	199.93	0.1810	38.1867
3.5	410.09	0.0280	43.7046

der Waals forces on inter and intramolecular chitosan. When chitosan is dissolved in acetic acid, H⁺ acetic acid interact with amino group (NH₂) chitosan and produces the NH₃⁺ cation. The NH₃⁺ cation triggers a repulsive force between the chitosan polymer chains, breaking some hydrogen bonds and other physical interactions at intra- and intermolecular chitosan (SOGIAS et al., 2010).

At low concentrations (2.5%), LMWC molecules have large intermolecular distances, lesser physical interactions between molecules, more protonated amine groups, and higher density cross-linking interaction with TPP anion (FAN et al., 2012). The excess protonated amino groups formed stable positively charged nanoparticles that could prevent large aggregate establishment (QUIÑONES et al., 2018). The small value of PDI (0.009) confirmed the narrow distribution and stability of nanoparticles (MASARUDIN et al., 2015) formed by 2.5% LMWC.

In contrast with low concentration, at higher concentration (3.5%), LMWC molecules have small intermolecular distance, have more physical interactions between molecules, less protonated amine group formed, and low repulsive force impacting low density cross-linking of interaction with TPP anion (FAN et al., 2012). At this concentration, TPP anions are more dominant than protonated amino. The exceed TPP anions formed negatively charged nanoparticles that stable and prevented particles aggregation (QUIÑONES et al., 2018). The small density of cross-linked interactions at high concentration (3.5%) initiated to form swollen particles, compared with a low concentration of LMWC (2.5%), which has high cross-linked interactions led to form more-compact nanoparticles (HUANG et al., 2015).

While at 3.0% LMWC, the LMWC molecules approached each other, hydrogen bonds between the LMWC molecules and the repulsive force stimulated by the NH₃⁺ cation are in a balanced state (FAN et al., 2012). Consequently, no negative or positive charge overwhelms to stabilize the particles,

and aggregate particles are formed (QUIÑONES et al., 2018). The PDI values of 3.0% LMWC are more significant than the other concentrations, showing that particle size has an extensive distribution (MASARUDIN et al., 2015).

The concentration of LMWC also affects to encapsulation efficiency of drugs. The LMWC molecules involved in cross-linking with TPP have interacted with poloxamer, which was physically bound to ETX before interacting with TPP. Consequently, the more LMWC molecules involved in cross-linking interactions with TPP and LMWC nanoparticles load more drugs. Based on stability, particle size, and encapsulation efficiency, it is known that chitosan with a concentration of 3.0% is the optimum concentration.

Influence of poloxamer 188 concentration on character of ETX-LMWC-NPs

Chitosan is a polymer that is not amphiphilic, so to load hydrophobic drugs such as ETX, a surfactant is required. The addition of surfactants will form oil micelles in water (o/w). The hydrophobic drug is at the core, and chitosan as a hydrophilic polymer is on the outer side (MOTIEI & KASHANIAN, 2017). In this study, non-ionic surfactant poloxamer 188 (Pluronic (F68)) was used. Poloxamer 188 has been used in chitosan nanoparticles synthesis for encapsulating drugs. The hydrophilic and lipophilic balance (HLB) value of poloxamer 188 (HLB = 29) makes poloxamer capable of stabilizing the suspension of chitosan nanoparticles (RASYID et al., 2014). Furthermore, several studies have been used poloxamer 188 as an excipient to elevate solubility of ETX (KAREKAR et al., 2009) suspension stabilizer and coat the drug-loaded NPs/MPs to help them to reach the target site (SHUBHRA et al., 2014).

The results in table 3 show that the ETX-LMWC-NPs without poloxamer 188 had the largest mean particle size (796.25 nm). In contrast,

Table 3 - Influence of Poloxamer 188 concentration to character of ETX-LMWC-NPs.

Poloxamer 188 (mg/mL)	Mean particle size (nm)	PDI	Encapsulation efficiency (%)
0	796.25	0.041	42.7695
1	178.86	0.009	35.1007
1.5	281.20	0.003	53.1665
2.0	391.66	0.040	59.3297

ETX-LMWC-NPs with poloxamer 188 have a lower particle size range from 178-391 nm. This phenomenon also was reported by LIU & HO (2017) with different concentrations of formulas and particle size. The resulting large particle size in the mixture without poloxamer 188 is the impact of particle aggregation triggered by the instability of the particles formed. In this case, the surfactant worked as a stabilizer by reducing surface tension and preventing aggregation (SUGITA et al., 2011). However, when poloxamer 188 increased to 2 mg/mL, a large number of micelles were formed and induced an osmotic force surrounding the nanoparticles. Osmotic force led nanoparticles to close each other. Nevertheless, the PEO of poloxamer that adsorbs the surface of LMWC-NPs prevents the nanoparticles from merging. Therefore, depletion flocculation occurs and results in nanoparticles aggregates with bigger particle sizes (WULFF-PÉREZ et al., 2009).

Furthermore, increasing the concentration of poloxamer 188 also increased the efficiency of ETX encapsulation in LMWC nanoparticles (Table 3). The result complies with the study reported by SUGITA et al. (2011) that the addition of non-ionic surfactants with high HLB values would raise the efficiency of drug encapsulation and the number of chitosan nanoparticles formed. A high HLB indicated that the surfactant is more hydrophilic, which can adsorb hydrophobic surfaces and form a coat that protects hydrophobic droplets to prevent aggregation (PAVONI et al., 2020). In this study, ETX in ethanol is hydrophobic while LMWC in acetic acid is hydrophilic. The polypropylene oxide (PPO) block of poloxamer 188 is capable of interacting with the hydrophobic drug. In contrast, the polyethylene oxide (PEO) block of poloxamer has a weak interaction with hydrophobic drugs and extends outside the hydrophobic surface of to interact with hydrophilic molecules (BODRATTI & ALEXANDRIDIS, 2018; SHUBHRA et al., 2014).

A significant quantity of poloxamer 188 provides more ETX and chitosan molecules involved in cross-linking interactions with TPP anions, thereby causing particle size and encapsulation efficiency enhancement. Based on the research results, the poloxamer 188 concentration of 1.5 mg/mL is the optimum concentration to obtain narrow distributed LMWC nanoparticles with a considerable value of drug efficiency encapsulation.

ETX-LMWC-NPs optimization result

This study optimized the formula to form ETX-LMWC-NPs and evaluated the effect of independent variables (LMWC concentration, LMWC/TPP mass ratio, and poloxamer 188 concentration) on dependent variables (particle size, PDI, and encapsulation efficiency). The optimization of ETX-LMWC-NPs was carried out using RSM and analyzed as statistical using Design Expert 13. The response of the combination of the independent variables is shown in table 4.

Mean particle size

Table 4 shows the particle size of 15 BBD formulas, ranging from 178.86 to 432.33 nm. Based on two-way ANOVA followed by multiple regression analysis performed on Design Expert 13, the recommended model for particle size response is Reduced-Two Factor Interactions (2FI) with significance p-value, insignificant lack of fit and determinant coefficient (R^2) 0.4984. A model reduction 2FI for particle size is shown that only concentration of LMWC (A) and poloxamer 188 (C) that significant effect to mean particle size (P-value < 0.05). The value of R^2 indicates that LMWC and poloxamer 188 concentration affects 49.84% of particle size. In comparison, the other 50.16% come from other independent variables outside the experimental parameter. The interaction between LMWC and poloxamer 188 concentration

Table 4 - Response data based on Box-Behnken Design towards mean particle size (Y_1), PDI (Y_2) and Efficiency encapsulation (Y_3).

Formula	-----Variable independent-----			-----Response-----		
	A	B	C	Y_1	Y_2	Y_3
1	3.5	5.5	1.5	353.27	0.052	37.4339 ± 1.04
2	2.5	4.5	1.0	178.86	0.009	38.9580 ± 1.42
3	2.5	3.5	1.5	332.49	0.022	35.7875 ± 1.88
4	3.5	3.5	1.5	373.37	0.023	39.3540 ± 2.94
5	3.0	4.5	1.5	322.75	0.076	45.2794 ± 1.33
6	3.0	5.5	2.0	294.5	0.085	50.1155 ± 0.07
7	3.5	4.5	2.0	354.92	0.025	47.2417 ± 1.45
8	3.0	3.5	2.0	335.71	0.160	42.3080 ± 2.06
9	2.5	5.5	1.5	318.11	0.144	46.1379 ± 1.15
10	3.0	4.5	1.5	328.22	0.080	43.9520 ± 0.68
11	2.5	4.5	2.0	391.66	0.040	38.3663 ± 0.33
12	3.0	5.5	1.0	270.67	0.090	45.4543 ± 1.45
13	3.5	4.5	1.0	410.09	0.028	43.6202 ± 0.12
14	3.0	4.5	1.5	432.33	0.829	49.1477 ± 2.88
15	3.0	3.5	1.0	414.63	0.036	40.6088 ± 0.92

Note: A = LMWC (%); B = LMWC/TPP mass ratio; C = Poloxamer 188 (mg/mL).

is exhibited in mathematical equation (2) and surface contour (Figure 1).

From figure 1, it could be seen that the smallest mean size particles were formed by 2.5% LMWC and 1.0 mg/mL poloxamer 188 and particle size enlarged with increasing LMWC and poloxamer 188 concentration. Escalating LMWC concentrate causes the reduction of distance between chitosan molecules, impacting many chitosan molecules involved in cross-linked interactions, forming grander particle size (FAN et al., 2012). Meanwhile, when the concentration of poloxamer 188 increased, the excess micelles formed and induced an osmotic force surrounding the nanoparticles that led nanoparticles to close each other. However, the PEO layer on the surface of LMWC-NPs prevents the nanoparticles from merging and triggers depletion-flocculation, resulting in nanoparticles aggregates with bigger particle sizes (WULFF-PÉREZ et al., 2009).

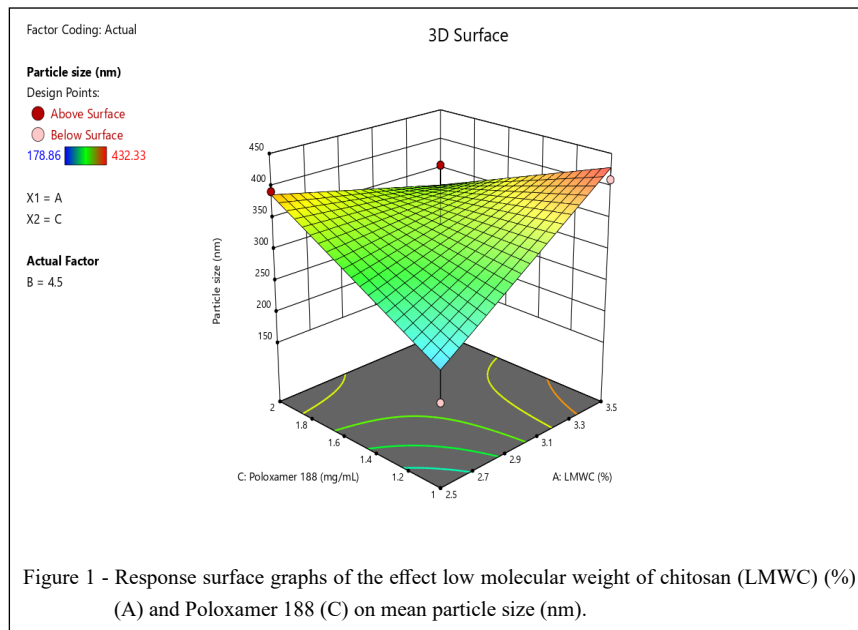
Polydispersity index (PDI)

Fifteen BBD formulas exhibited PDI range from 0.009 to 0.829. An enormous polydispersity

index value indicates a wide variety of particle size distributions. The reason is the instability of the particles produced, resulting in aggregation and non-uniformity of particles (MASARUDIN et al., 2015). The results of the ANOVA test showed that the mean model is fit with the polydispersity index response with a value of 0.1133 and a sequential p-value of 0.0485 without any R^2 value. The results of the ANOVA test showed that LMWC concentration (A), the LMWC/TPP mass ratio (B), and poloxamer 188 concentration (C) did not have a significant effect on the PDI of nanoparticles. The model's suitability was confirmed by the non-significant value of lack of fit 0.9921 (P-value > 0.05). There is no mathematical equation for the mean model.

Encapsulation efficiency

Based on the results of the ANOVA test, it is known that the fit polynomial model for encapsulation efficiency data is the Reduced-Quadratic model (P-value < 0.05) with an insignificant lack of fit and R^2 value 0.6483. This model only presented LMWC concentration (A) and LMWC/TPP mass ratio (B) as



variables that significantly affect the encapsulation efficiency ($P < 0.05$). The interaction between LMWC and LMWC/TPP mass ratio to encapsulation efficiency were displayed in mathematical equation (3) and a three-dimensional surface graph (Figure 2). Relied on figure 2, it is known that the highest encapsulation efficiency is found at a concentration of 3% LMWC and increases with the increase in the mass ratio of LMWC/TPP. The mass ratio of large LMWC/TPP has a minimum TPP concentration, resulting in lower $\text{NH}_3^+-\text{P}_3\text{O}_{10}^{5-}$ cross-linked density, impacting form swollen nanoparticles (HUANG et al. 2015) load more ETX.

$$\text{Encapsulation efficiency} = 45.27 + 1.05 A + 2.63 B - 3.07 AB - 4.40 A^2 \quad (3)$$

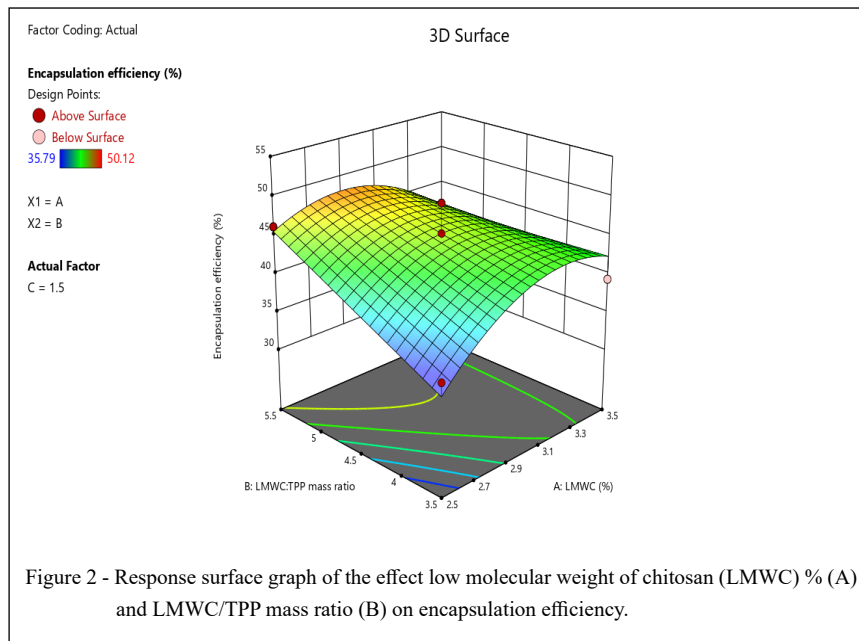
Optimization and verification of optimum character of ETX-LMWC-NPs

The optimization variables by Design Expert 13 software obtained a formula with the desirability value of 0.797, indicating the formula predicted will form the desired character of nanoparticle as much 79.7%. The optimum formula consists of LMWC 2.659%, a mass ratio of LMWC/TPP of 5.5, and 1 mg/mL poloxamer 188. Observation results with the optimum formula (Table 5) reported that chitosan nanoparticles have a mean particle size of 259.91 nm, PDI of 0.040, and encapsulation efficiency of 51.252%. The PDI and encapsulation efficiency observational data are not entirely similar

to the predicted data provided by the Design Expert 13 software. However, the observed data are still in the 95% range of Confident-Interval (CI) and Prediction-Interval (PI). Therefore, the mathematical equations obtained are still good enough to determine the optimal formula and the expected sensory response. The differences between observed data and predicted data are influenced by several factors: the nanoparticle synthesis process, storage conditions, and measurement (PATRA & BAEK, 2014).

Morphology of LMWC-ETX-NPs

Photographs of ETX-LMWC-NPs with 2000x and 1000x magnification (Figure 3) show that ERX-LMWC-NPs have a spherical shape with non-uniform sizes. The particle size and its distribution on the SEM photograph are not imaging the result from the PSA instrument. The drying process of the nanosuspension using a spray dryer and instability nanoparticle powder could lead to this phenomenon. Inappropriate drying conditions of nanoparticle suspension were reported to increase the polydispersity index and particle size (MOHAJEL et al., 2012). The particle size increases with temperature and air velocity elevation in the spray drying apparatus (WEI et al., 2020). Moreover, the LMWC reported has a high swelling degree (GUPTA & JABRAIL, 2007), hygroscopic properties (SZYMAŃSKA & WINNICKA, 2015), and low deacetylation degree,



which led to more absorption of water and particle size enhancement during storage.

Functional group of ETX-LMWC-NPs

To achieve information of any changes in the chemical structure of LMWC and ETX during the formation of nanoparticles. FTIR spectra of LMWC, ETX loaded LMWC nanoparticles, and ETX were recorded and compared in figure 4. The main characteristics of chitosan spectrum were observed in the spectra of LMWC, LMWC-NPs, and ETX-LMWC-NPs, such as broadband absorption between 3500-3000 cm⁻¹ (O-H and N-H groups of primary amines); 2927 and 2880 cm⁻¹ (C-H group); the spectrum peak at 1715 cm⁻¹ (C=O group of the

amide I); the spectrum peak in the area of 1643–1572 cm⁻¹ (a bent N-H group of the primary amine); the absorption peak in the area of 1428 cm⁻¹ (bent CH₂ groups) and; the absorption peak in the 1154 cm⁻¹ (the asymmetric strain of the C-O-C bridge glycosidic bond) (SILVESTRO et al., 2020). Strain peak at 1069 cm⁻¹ (a chitosan skeleton vibration involving the O-C-O) and 1020 cm⁻¹ (the polysaccharide absorption band) similar to that reported by the previous studies (ISLAM et al., 2019).

The FTIR ETX spectrum showed a characteristic peak; the absorption at 1598 cm⁻¹ was associated with the stretching vibration of C=N; 1496 cm⁻¹, 1286 cm⁻¹, 1130 cm⁻¹, and 1085 cm⁻¹ were associated with S=O stretching vibrations.

Table 5 - Verification of ETX-LMWC-NPs characters resulted from optimum formula based on *Design Expert 13* program.

Response	-----Optimum formula-----					
	Prediction	Observation	95 % CI low	95 % CI high	95 % PI low	95 % PI high
Mean particle size (nm)	259.203	259.91	88.34	319.78	128.035	390.371
PDI	0.113	0.040	0.0008	0.225	-0.336	0.562
Encapsulation efficiency (%)	47.2311	51.252	43.5860	51.4994	41.4938	52.9684

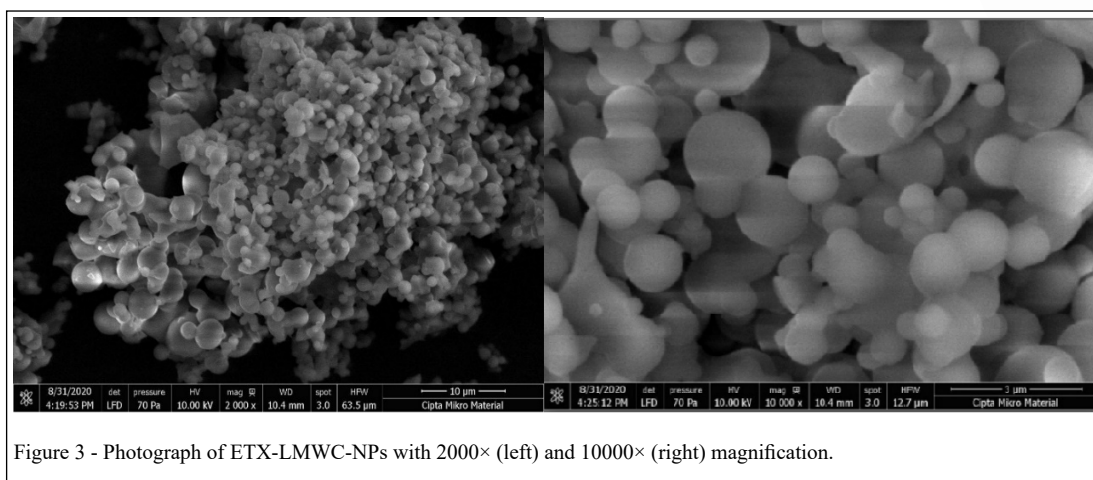


Figure 3 - Photograph of ETX-LMWC-NPs with 2000× (left) and 10000× (right) magnification.

Meanwhile, the absorption at 839 cm^{-1} , 771 cm^{-1} and 635 cm^{-1} were relative to the C-Cl strain vibration (ARUNKUMAR et al., 2016; DAS et al., 2011).

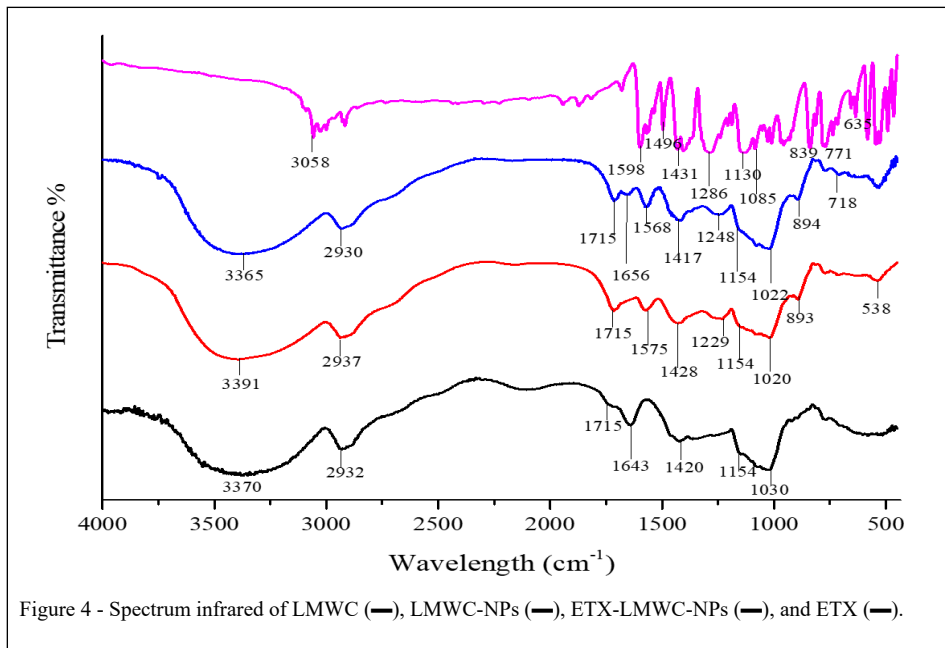
There are differences in wavenumber, intensity, and peak characteristic bands typical of TPP in LMWC-NPs and ETX-LMWC-NPs spectra. The wavenumbers of the O-H and N-H regions have shifted from 3370 cm^{-1} at LMWC to 3390 cm^{-1} at LMWC-NPs. The displacement of wavenumber is an outcome of an additional O-H group from poloxamer 188. In contrast to O-H peak in the LMWC spectrum, O-H group wavenumber of ETX-LMWC-NPs has a smaller value, owing to the hydrogen bond between OH with SO_2 and N-pyridine of ETX (KAREKAR et al., 2009). Before being used to form nanoparticles, the difference observed in the primary amine group (N-H) bend region at 1643 cm^{-1} for LMWC. However, after the formed nanoparticle, the wavenumber shifted became 1578 and 1568 cm^{-1} for LMWC-NPs and ETX-LMWC-NPs with lesser intensity. Electrostatic interaction of primary amine group (NH_3^+) with TPP polyanions encourages wavenumber shifting (LUO et al., 2010) and intensity reduction (SILVESTRO et al., 2020). The phenomenon confirmed the formation of nanoparticles through interaction between NH from LMWC and TPP.

The existence of TPP in nanoparticles was also confirmed by absorption band at 1229 cm^{-1} (LMWC-NPs) and 1248 cm^{-1} (ETX-LMWC-NPs) regions identified as P=O and absorption 894 cm^{-1} regions specified as P-O-P from TPP. The presence of ETX in ETX-LMWC-NPs was noticed from the absorption band at 1656 cm^{-1} and 718 cm^{-1} regions, which were identified as C=N and C-Cl stretching

vibration, respectively. Both absorptions are not found in LMWC-NPs.

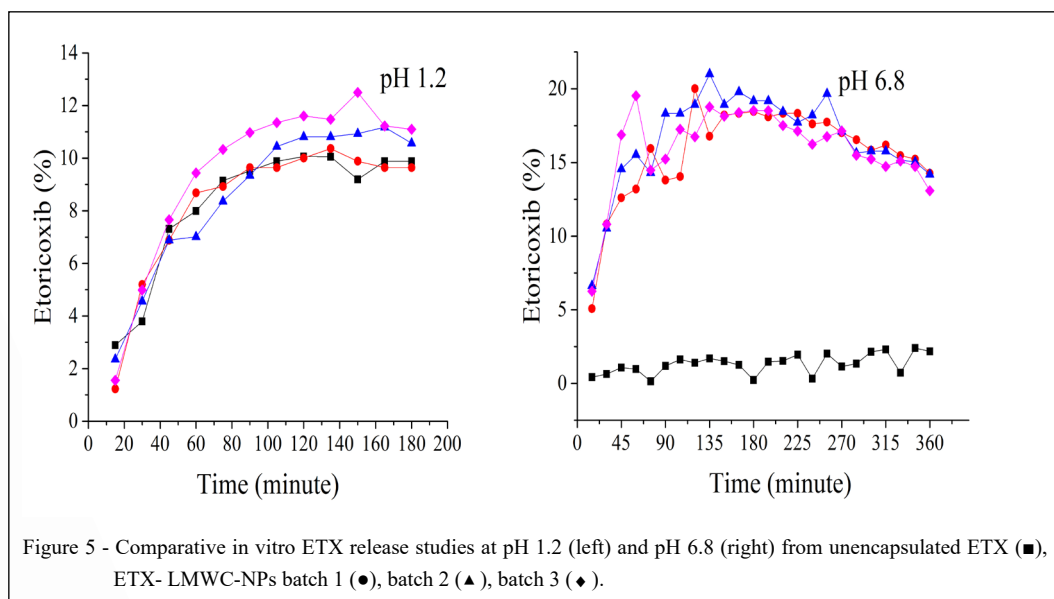
In-Vitro Release Study

The ETX release profile from LMWC-NPs was determined in-vitro in the medium solution with pH and temperature ($37\text{ }^\circ\text{C}$) similar to gastric juice (pH 1.2) and intestinal liquid (pH 6.8). The result is shown in figure 5. The release rates of encapsulated and unencapsulated ETX at pH 1.2 are not significantly different. In contrast, at pH 6.8, unencapsulated ETX has a slow and small amount of release, only 1-2%, which is significantly different with encapsulated ETX up to 19% ETX reported has higher solubility in pH 1.2 and poor solubility at pH 6.8 (ASHOKRAJ et al., 2016). ETX encapsulation by LMWC-NPs showed improvement of the ETX solubility and dissolution in pH 6.8 medium. The water-soluble property of LMWC and poloxamer 188 used in the form of ETX-LMWC-NPs enhance the solubility and release rate of ETX at pH 6.8. The release rate profile of ETX from ETX-LMWC-NPs in both mediums (pH 1.2 and pH 6.8) showed initial burst release up to 9% at pH 1.2 medium and 19% in base medium till first 60th minutes. Furthermore, ETX was released at a slow rate until it reached a maximum value of 10-12% in 150th minutes and showed steady release (8-10%) until 180th minutes at pH 1.2. While at pH 6.8 medium, ETX release has maximum release at 21% in 135th minute and decreases gradually and slowly until it reaches 10-14% in 360th minute. However, in both mediums, ETX release did not reach the maximum total of ETX that was used in the study.



Initial burst release in acid and base medium could be led by weakly bonded or adsorbed of the drugs on the surface of nanoparticles (SINGH & LILLARD JR., 2009). Moreover, LMWC has a high swelling degree and fragile network structure, which impacted to poor retention of ETX (GUPTA & JABRAIL, 2007). In contrast, the slow-release could

be influenced by the ETX molecules more entrapped and tightly bound by the LMWC molecules or infected by the dialysis sac method used in this research. LMWC polymer and cellulose membrane (dialysis sac) may experience a swelling process and form a gel when soaked into a medium solution. Consequently, the dialysis sac method will add diffusion path length,



so it takes a long time for ETX to reach the receiver compartment (VARMA et al., 2004).

Conversely, the previous study reported that cellulose could interact with chitosan (ROHAETI et al. 2018), so the LMWC-NPs in the dialysis sac tended to accumulate the cellulose membrane surface, causing particle aggregation at the surface of the membrane and destabilization (WENG et al. 2020). As a result, ETX had burst-release, continued by slow-release, and gradually decreased. Agitation inadequate inside the dialysis sac also could be another factor of ETX incomplete release from LMWC-NPs. Due to the hindrance of ETX to drug diffusion through the dialysis membrane, it confirmed that the dialysis membrane method could not critically explain the ETX dissolution of nanoparticles (SHEN & BURGESS, 2013; WENG et al., 2020).

Kinetic model equations such as zero-order, first-order, Higuchi's, Hixson-Crowell, and Korsmeyer-Peppas equation were observed and written in table 6 to determine the appropriate model dissolution kinetics. Based on the determination coefficient value (R^2), it was seen in table 6 that both medium approach Korsmeyer-Peppas model with $R^2 = 0.8373$ at pH 1.2 and $R^2 = 0.4322$ at pH 6.8. Korsmeyer-Peppas model equation also could predict the mechanism of ETX release from exponent release (n) value. Based on the exponent release of a spherical sample by RITGER & PEPPAS (1987), it could be seen that ETX release at pH 1.2 had anomalous (non-Fickian) transport ($n = 0.6545$) that indicated the combination of erosion

and diffusion of polymer in ETX release mechanism (SHAH & KHAN, 2012). Different with pH 6.8 had n value less than 0.43 (0.1924) corresponding to lower Fickian diffusion or quasi Fickian. The obtained n value of ETX release at pH 6.8 is probably influenced by wide distribution of particles (RITGER & PEPPAS, 1987) due to the spray drying method and hygroscopic properties of LMWC.

CONCLUSION

The optimum formula to obtain ETX-LMWC-NPs with the smallest average particle size, low PDI and the highest encapsulation efficiency is 2.659% LMWC, 5.5 LMWC/TPP ratio and 1 mg/mL poloxamer 188. Based on this formula, we found ETX-LMWC-NPs with mean particle size of 259.91 nm with PDI of 0.040 and ETX encapsulation efficiency of 51.25%. SEM photographs showed ETX-LMWC-NPs have spherical form and aggregated. Characterization by FTIR showed there was no chemical interaction between ETX and LMWC. The presence of ETX in ETX-LMWC-NPs was confirmed by the absorption peak of C=N and C-Cl group at 1658 cm^{-1} and 718 cm^{-1} , respectively. ETX release kinetics from ETX-LMWC-NPs at pH 1.2 and pH 6.8 solution, approached to Korsmeyer-Peppas kinetic model, with a maximum release percentage of 10-12% pH 1.2 and 20-21% at pH 6.8. ETX encapsulation with LMWC-NPs increased the solubility and dissolution of ETX up to 19% at medium pH 6.8.

Table 6 - ETX release kinetic from ETX-LMWC-NPs in acid (pH 1.2) and alkaline (pH 6.8) medium.

Drug release kinetics model	ETX-LMWC-NPs in pH 1.2	ETX-LMWC-NPs in pH 6.8
Zero order $Q = kt$	$y = 0.045x + 4.4105$ $R^2 = 0.7068$	$y = 0.0079x + 14.609$ $R^2 = 0.0826$
First order $\ln[A]_t = \ln[A]_0 - kt$	$y = -5 \times 10^{-4}x - 0.4566$ $R^2 = 0.7147$	$y = -9 \times 10^{-5}x - 0.5708$ $R^2 = 0.0776$
Higuchi $Q = kt^{1/2}$	$y = 0.8388x + 0.5211$ $R^2 = 0.8346$	$y = 0.2966x + 12.232$ $R^2 = 0.1962$
Hixson-Crowell $Q_0^{1/3} - Q_t^{1/3} = kt$	$y = -1 \times 10^{-4}x + 0.8588$ $R^2 = 0.7121$	$y = -2 \times 10^{-5}x + 0.8269$ $R^2 = 0.0793$
Korsmeyer-Peppas $Q = kt^n$	$y = 0.6545x - 0.3399$ $R^2 = 0.8373$	$y = 0.1924x - 0.7795$ $R^2 = 0.4322$

ACKNOWLEDGEMENTS

The ETX was given by PT. Dexa Medica Indonesia. The authors would like to thank all analysts in the present research and IPB university for allowing us to use the laboratory.

DECLARATION OF CONFLICT OF INTEREST

The authors declare no conflict of interest. The founding sponsors had no role in the design of the study, in the collection, analyses, or interpretation of data, in the writing of the manuscript, and in the decision to publish the results.

AUTHORS' CONTRIBUTIONS

All authors contributed equally for the conception and writing of the manuscript. All authors critically revised the manuscript and approved of the final version.

REFERENCES

- AGRAWAL, N. G. B. et al. Dose proportionality of oral etoricoxib, a highly selective cyclooxygenase-2 inhibitor, in healthy volunteers. **Journal of Clinical Pharmacology**, 2001. v. 41, n. 10, p. 1106–1110. Available from: <<https://doi.org/10.1177/0091270003251122>>. Accessed: Aug. 12, 2019.
- ANTONIOU, J. et al. Physicochemical and morphological properties of size-controlled chitosan-tripolyphosphate nanoparticles. **Colloids and Surfaces A: Physicochemical and Engineering Aspects**, 2015. v. 465, p. 137–146. Available from: <<http://dx.doi.org/10.1016/j.colsurfa.2014.10.040>>. Accessed: Aug. 12, 2019.
- ARUNKUMAR, P. et al. Synthesis, characterizations, in vitro and in vivo evaluation of Etoricoxib-loaded Poly (Caprolactone) microparticles-a potential Intra-articular drug delivery system for the treatment of Osteoarthritis. **Journal of Biomaterials Science, Polymer Edition**, 2016. v. 27, n. 4, p. 303–316. Available from: <<http://doi.org/10.1080/09205063.2015.1125564>>. Accessed: Jun. 5, 2020.
- ASHOKRAJ, Y. et al. Discriminatory dissolution method development and validation of etoricoxib tablets. **Dissolution Technologies**, 2016. v. 23, n. 2, p. 30–34. Available from: <<http://doi.org/10.14227/DT230216P30>>. Accessed: Aug. 23, 2021.
- BIRMINGHAM, B.; BUVANENDRAN, A. Nonsteroidal anti-inflammatory drugs, acetaminophen, and COX-2 inhibitors. *In: BENZON, H. T. et al. (Org.). Practical Management of Pain*. Fifth Edit ed. Amsterdam: Elsevier Inc., 2013, p. 553–568.
- BODRATTI, A. M.; ALEXANDRIDIS, P. Formulation of poloxamers for drug delivery. **Journal of Functional Biomaterials**, 2018. v. 9, n. 11, p. 1–24. Available from: <<http://doi.org/10.3390/jfb9010011>>. Accessed: Sep. 5, 2021.
- BOGUSZ, K. et al. Synthesis of methotrexate-loaded tantalum pentoxide-poly(acrylic acid) nanoparticles for controlled drug release applications. **Journal of Colloid and Interface Science**, 2019. v. 538, p. 286–296. Available from: <<https://doi.org/10.1016/j.jcis.2018.11.097>>. Accessed: Jul. 12, 2021.
- CROOM, K. F.; SIDDIQUE, M. A. A. Etoricoxib a review of its Use in the Symptomatic Treatment of Osteoarthritis, Rheumatoid Arthritis, Ankylosing Spondylitis and Acute Gouty Arthritis. **Drugs**, 2009. v. 69, n. 11, p. 1513–1532. Available from: <<http://doi.org/10.2165/00003495-200969110-00008>>. Accessed: Aug. 11, 2020.
- DANAELI, M. et al. Impact of Particle Size and Polydispersity Index on the Clinical Applications of Lipidic Nanocarrier Systems. **Pharmaceutics**, 2018. v. 10, n. 57, p. 1–17. Available from: <<http://doi.org/10.3390/pharmaceutics10020057>>. Accessed: Jan. 21, 2021.
- DAS, A. et al. Solubility and Dissolution Enhancement of Etoricoxib by Solid Dispersion Technique Using Sugar Carriers. **ISRN Pharmaceutics**, 2011. v. 2011, n. Peg 4000, p. 1–8. Available from: <<https://doi.org/10.5402/2011/819765>>. Accessed: Jun. 10, 2020.
- ESCUADERO-CONTRERAS, A.; CERVANTES, J. V. M.; COLLANTES-ESTEVEZ, E. **Update on the clinical pharmacology of etoricoxib, a potent cyclooxygenase-2 inhibitor**. **Future Rheumatology**. 2007. Available from: <<http://doi.org/10.2217/17460816.2.6.545>>. Accessed: Jul. 13, 2020.
- FAN, W. et al. Formation mechanism of monodisperse, low molecular weight chitosan nanoparticles by ionic gelation technique. **Colloids and Surfaces B: Biointerfaces**, 2012. v. 90, n. 1, p. 21–27. Available from: <<http://dx.doi.org/10.1016/j.colsurfb.2011.09.042>>. Accessed: Aug. 3, 2019.
- FENG, X. et al. Gastrointestinal safety of etoricoxib in osteoarthritis and rheumatoid arthritis: A meta-analysis. **PLoS ONE**, 2018. v. 13, n. 1, p. 1–13. Available from: <<https://doi.org/10.1371/journal.pone.0190798>>. Accessed: Aug. 10, 2020.
- FRACON, R. N. et al. Treatment with paracetamol, ketorolac or etoricoxib did not hinder alveolar bone healing: a histometric study in rats. **Journal of Applied Oral Science**, 2010. v. 18, n. 6, p. 630–634. Available from: <<https://doi.org/10.1590/S1678-77572010000600016>>. Accessed: Nov. 4, 2021.
- GUPTA, K. C.; JABRAIL, F. H. Glutaraldehyde cross-linked chitosan microspheres for controlled release of centchroman. **Carbohydrate Research**, 2007. v. 342, n. 15, p. 2244–2252. Disponivel em: <<http://doi.org/10.1016/j.carres.2007.06.009>>. Acesso em: 3 set. 2021.
- HU, Z. et al. Investigation of the effects of molecular parameters on the hemostatic properties of chitosan. **Molecules**, 2018. v. 23, n. 12, p. 1–14. Available from <<http://doi.org/10.3390/molecules23123147>>. Accessed: Aug. 24, 2020.
- HUANG, Y.; CAI, Y.; LAPITSKY, Y. Factors affecting the stability of chitosan/tripolyphosphate micro- and nanogels: Resolving the opposing findings. **Journal of Materials Chemistry B**, 2015. v. 3, n. 29, p. 5957–5970. Available from: <<https://doi.org/10.1039/c5tb00431d>>. Accessed: Aug. 29, 2020.
- HWANG, H. Y. et al. Tumor targetability and antitumor effect of docetaxel-loaded hydrophobically modified glycol chitosan nanoparticles. **Journal of Controlled Release**, 2008. v. 128, n. 1, p. 23–31. Available from: <<http://doi.org/10.1016/j.jconrel.2008.02.003>>. Accessed: Jul. 8, 2020.
- INAMDAR, N. N.; MOURYA, V. Chitosan and low molecular Weight Chitosan: Biological and Biomedical Applications. *In:*

- TIWARI, A.; NORDIN, A. N. (Org.). **Advanced Biomaterials and Biodevices**. Beverly: Scrivener Publishing LLC, 2014, p. 183–242.
- ISLAM, N. et al. In vitro enzymatic digestibility of glutaraldehyde-crosslinked chitosan nanoparticles in lysozyme solution and their applicability in pulmonary drug delivery. **Molecules**, 2019. v. 24, n. 7, p. 1–17. Available from: <<http://doi.org/10.3390/molecules24071271>>. Accessed: Dec. 31, 2020.
- JONG, W. H. De; BORM, P. J. Drug delivery and nanoparticles: applications and hazards. **International Journal of Nanomedicine**, 2008. v. 3, n. 2, p. 133–149. Available from: <<https://doi.org/10.2147/IJN.S596>>. Accessed: Feb. 13, 2019.
- KAREKAR, P. et al. Physicochemical investigation of the solid dispersion systems of etoricoxib with poloxamer 188. **Pharmaceutical Development and Technology**, 2009. v. 14, n. 4, p. 373–379. Available from: <<https://doi.org/10.1080/10837450802683974>>. Accessed: Jun. 5, 2020.
- KAUR, G.; PALIWAL, S. Formulation and evaluation of Etoricoxib Microbeads for Sustained Drug Delivery. **Universal Journal of Pharmaceutical Research**, 2019. v. 4, n. 1, p. 35–39. Available from: <<https://doi.org/10.22270/ujpr.v4i1.241>>. Accessed: Aug. 17, 2020.
- KITA, K.; DITTRICH, C. **Drug delivery vehicles with improved encapsulation efficiency: Taking advantage of specific drug-carrier interactions**. **Expert Opinion on Drug Delivery**. 2011. Available from: <<https://doi.org/10.1517/17425247.2011.553216>>. Accessed: Aug. 17, 2020.
- KOUKARAS, E. N. et al. Insight on the formation of chitosan nanoparticles through ionotropic gelation with tripolyphosphate. **Molecular Pharmaceutics**, 2012. v. 9, n. 10, p. 2856–2862. Available from: <<https://doi.org/10.1021/mp300162j>>. Accessed: Jul. 20, 2019.
- LEE, M. et al. Water-soluble and low molecular weight chitosan-based plasmid DNA delivery. **Pharmaceutical Research**, 2001. v. 18, n. 4, p. 427–431. Available from: <<https://doi.org/10.1023/A:1011037807261>>. Accessed: Aug. 16, 2020.
- LI, Jiahua et al. Chitosan-Based Nanomaterials for Drug Delivery. **Molecules**, 2018. v. 23, n. 10, p. 2661. Available from: <<http://www.mdpi.com/1420-3049/23/10/2661>>. Accessed: Mar. 29, 2019.
- LIU, S.; HO, P. C. Formulation optimization of scutellarin-loaded HP- β -CD/chitosan nanoparticles using response surface methodology with Box–Behnken design. **Asian Journal of Pharmaceutical Sciences**, 2017. v. 12, n. 4, p. 378–385. Available from: <<http://dx.doi.org/10.1016/j.ajps.2017.04.003>>. Accessed: Jun. 28, 2020.
- LUO, Y. et al. Preparation, characterization and evaluation of selenite-loaded chitosan/TPP nanoparticles with or without zein coating. **Carbohydrate Polymers**, 2010. v. 82, n. 3, p. 942–951. Available from: <<http://dx.doi.org/10.1016/j.carbpol.2010.06.029>>. Accessed: May. 21, 2020.
- MALVIYA, R.; SHARMA, P. K.; DUBEY, S. K. Efficiency of self-assembled etoricoxib containing polyelectrolyte complex stabilized cubic nanoparticles against human cancer cells. **Precision Medical Sciences**, 2020. v. 9, n. 1, p. 9–22. Available from: <<https://doi.org/10.1002/prm2.12004>>. Accessed: Aug. 16, 2020.
- MASARUDIN, M. J. et al. Factors determining the stability, size distribution, and cellular accumulation of small, monodisperse chitosan nanoparticles as candidate vectors for anticancer drug delivery: application to the passive encapsulation of [14 C]-doxorubicin. **Nanotechnology, Science and Applications**, 2015. v. 8, p. 67–80. Available from: <<https://pdfs.semanticscholar.org/e414/f2a7637a19a4ef1e2211af2b70c25e86d2d4.pdf>>. Accessed: May. 13, 2019.
- MOHAJEL, N. et al. Drying of a plasmid containing formulation: Chitosan as a protecting agent. **DARU, Journal of Pharmaceutical Sciences**, 2012. v. 20, n. 1, p. 1–9. Available from: <<https://doi.org/10.1186/2008-2231-20-29>>. Accessed: Nov. 24, 2020.
- MOTIEI, M.; KASHANIAN, S. Preparation of amphiphilic chitosan nanoparticles for controlled release of hydrophobic drugs. **Journal of Nanoscience and Nanotechnology**, 2017. v. 17, n. 8, p. 5226–5232. Available from: <<https://doi.org/10.1166/jnn.2017.13844>>. Accessed: Oct. 21, 2020.
- NASKAR, S.; SHARMA, S.; KUOTSU, K. Chitosan-based nanoparticles: An overview of biomedical applications and its preparation. **Journal of Drug Delivery Science and Technology**, 2019. v. 49, n. 2019, p. 66–81. Available from: <<https://doi.org/10.1016/j.jddst.2018.10.022>>. Accessed: Aug. 22, 2020.
- PATEL, H. M. et al. Preparation and characterization of etoricoxib- β -cyclodextrin complexes prepared by the kneading method. **Acta Pharm**, 2007. v. 57, p. 351–359. Available from: <<https://doi.org/10.2478/v10007-007-0028-2>>. Accessed: Aug. 14, 2020.
- PATRA, J. K.; BAEK, K. H. **Green Nanobiotechnology: Factors Affecting Synthesis and Characterization Techniques**. **Journal of Nanomaterials**. Available from: <<http://doi.org/10.1155/2014/417305>>. Accessed: Nov. 23, 2020.
- PAVONI, L. et al. An overview of micro- and nanoemulsions as vehicles for essential oils: Formulation, preparation and stability. **Nanomaterials**, 2020. v. 10, n. 1. Available from: <<https://doi.org/10.3390/nano10010135>>. Accessed: 6, 2021.
- QUIÑONES, J. P.; PENICHE, H.; PENICHE, C. Chitosan based self-assembled nanoparticles in drug delivery. **Polymers**, 2018. v. 10, n. 3, p. 1–32. Available from: <<https://doi.org/10.3390/polym10030235>>. Accessed: 2, 2019.
- RASYID, N. Q. et al. Suspension Stability and Characterization of Chitosan Nanoparticle-Coated Ketoprofen Based on Surfactants Oleic Acid and Poloxamer 188. **Makara Journal of Science**, 10 set. 2014. v. 18, n. 3. Available from: <<https://doi.org/10.7454/mss.v18i3.3720>>. Accessed: May. 3, 2019.
- RITGER, P. L.; PEPPAS, N. A. A simple equation for description of solute release i. Fickian and non-fickian release from non-swelling devices in the form of slabs, spheres, cylinders or discs. **Journal of Controlled Release**, 1987. v. 5, p. 23–36. Available from: <[https://doi.org/10.1016/0168-3659\(87\)90034-4](https://doi.org/10.1016/0168-3659(87)90034-4)>. Accessed: Sep. 2, 2021.
- ROHAETI, E.; LAKSONO, E. W.; RAKHMAWATI, A. Mechanical Properties and Antibacterial Activity of Cellulose Composite based Coconut Water with Addition of Glycerol, Chitosan, and Silver Nanoparticle. **Oriental Journal of Chemistry**, 2018. v. 34, n. 3, p. 1341–1349. Available from: <<https://doi.org/10.13005/ojc/340320>>. Accessed: Sep. 2, 2021.

- SASICH, L. D.; BARASAIN, M. A.; KUDSI, M. A. AL. **The cardiovascular risks of etoricoxib (Arcoxia).** *Annals of Saudi Medicine*, 2008. Available from: <<https://doi.org/10.4103/0256-4947.51740>>. Accessed: Aug. 24, 2020.
- SHAH, K. U.; KHAN, G. M. Regulating drug release behavior and kinetics from matrix tablets based on fine particle-sized ethyl cellulose ether derivatives: An in vitro and in vivo evaluation. *The Scientific World Journal*, 2012. v. 2012, p. 1–8. Available from: <<https://doi.org/10.1100/2012/842348>>. Accessed: Sep. 3, 2021.
- SHANG, L.; NIENHAUS, K.; NIENHAUS, G. U. **Engineered nanoparticles interacting with cells: Size matters.** *Journal of Nanobiotechnology*. Journal of Nanobiotechnology. Available from: <<https://doi.org/10.1186/1477-3155-12-5>>. Accessed: Aug. 21, 2020.
- SHEN, J.; BURGESS, D. J. In Vitro Dissolution Testing Strategies for Nanoparticulate Drug Delivery Systems: Recent Developments and Challenges. *Drug Deliv Transl Res*, 2013. v. 3, n. 5, p. 409–415. Available from: <<https://doi.org/10.1007/s13346-013-0129-z>>. Accessed: Sep. 8, 2021.
- SHUBHRA, Q. T. H. et al. Poloxamers for surface modification of hydrophobic drug carriers and their effects on drug delivery. *Polymer Reviews*, 2014. v. 54, n. 1, p. 112–138. Available from: <<https://doi.org/10.1080/15583724.2013.862544>>. Accessed: Sep. 5, 2021.
- SILVESTRO, I. et al. Preparation and characterization of TPP-chitosan crosslinked scaffolds for tissue engineering. *Materials*, 2020. v. 13, n. 16, p. 1–15. Available from: <<https://doi.org/10.3390/MA13163577>>. Accessed: Nov. 24, 2020.
- SINGH, R.; LILLARD JR., J. W. Nanoparticle-based targeted drug delivery. *Exp Mol Pathol*, 2009. v. 86, n. 3, p. 215–223. Available from: <<http://pendientedemigracion.ucm.es/info/ec/jec7/pdf/com3-6.pdf>>. Accessed: Aug. 21, 2020.
- SOGIAS, I. A.; KHUTORYANSKIY, V. V.; WILLIAMS, A. C. Exploring the factors affecting the solubility of chitosan in water. *Macromolecular Chemistry and Physics*, 2010. v. 211, n. 4, p. 426–433. Available from: <<https://doi.org/10.1002/macp.200900385>>. Accessed: Jun. 14, 2020.
- SUGITA, P.; NAPHTALENI; KURNIATI, M.; WUKIRSARI, T. Enkapsulasi ketoprofen dengan kitosan-alginat berdasarkan jenis dan ragam konsentrasi tween 80 dan span 80. *MAKARA of Science Series*, 2010. v. 14, n. 2, p. 107–112. Available from: <<http://doi.org/10.7454/mss.v14i2.678>>. Accessed: Aug. 29, 2020.
- SUGITA, P.; AMBARSARI, L.; LIDINIYAH. Optimization of Ketoprofen-loaded Chitosan Nanoparticle Ultrasonication Process. *Procedia Chemistry*, 2015. v. 16, p. 673–680. Available from: <<https://doi.org/10.1016/j.proche.2015.12.007>>. Accessed: Aug. 12, 2019.
- SZYMAŃSKA, E.; WINNICKA, K. Stability of chitosan - A challenge for pharmaceutical and biomedical applications. *Marine Drugs*, 2015. v. 13, n. 4, p. 1819–1846. Available from: <<https://doi.org/10.3390/md13041819>>. Accessed: Jan. 20, 2019.
- TAKEMOTO, J. K. et al. Clinical Pharmacokinetic and Pharmacodynamic Profile of Etoricoxib. *Clinical Pharmacokinetics*, 2008. v. 47, n. 11, p. 703–720. Available from: <<https://doi.org/10.1007/s40262-017-0604-7>>. Accessed: Aug. 11, 2020.
- TIAN, Meng et al. Molecular weight dependence of structure and properties of chitosan oligomers. *RSC Advances*, 2015. v. 5, n. 85, p. 69445–69452. Available from: <<https://doi.org/10.1039/c5ra08358c>>. Accessed: Jan. 10, 2020.
- VARMA, M. V. S. et al. **Factors affecting mechanism and kinetics of drug release from matrix-based oral controlled drug delivery systems.** *American Journal of Drug Delivery*. Available from: <<https://doi.org/10.2165/00137696-200402010-00003>>. Accessed: Aug. 24, 2021.
- WAHID, A.; SRIDHAR, B.; SHIVAKUMAR, S. **Preparation and evaluation of transdermal drug delivery system of etoricoxib using modified chitosan.** *Indian Journal of Pharmaceutical Sciences*. Available from: <<https://doi.org/10.4103/0250-474X.44593>>. Accessed: Aug. 16, 2020.
- WANAT, K. Biological barriers, and the influence of protein binding on the passage of drugs across them. *Molecular Biology Reports*, 2020. v. 47, n. 4, p. 3221–3231. Available from: <<https://doi.org/10.1007/s11033-020-05361-2>>. Accessed: Aug. 14, 2020.
- WEI, Y. et al. Investigations of the influences of processing Conditions on the Properties of Spray Dried Chitosan-Tripolyphosphate Particles loaded with Theophylline. *Scientific Reports*, 2020. v. 10, n. 1, p. 1–12. Available from: <<https://doi.org/10.1038/s41598-020-58184-3>>. Accessed: Oct. 21, 2020.
- WENG, J.; TONG, H. H. Y.; CHOW, S. F. In vitro release study of the polymeric drug nanoparticles: Development and validation of a novel method. *Pharmaceutics*, 2020. v. 12, n. 8, p. 1–18. Available from: <<https://doi.org/10.3390/pharmaceutics12080732>>. Accessed: Nov. 26, 2020.
- WULFF-PÉREZ, M. et al. Stability of emulsions for parenteral feeding: Preparation and characterization of o/w nanoemulsions with natural oils and Pluronic f68 as surfactant. *Food Hydrocolloids*, 2009. v. 23, n. 4, p. 1096–1102. Available from: <<https://doi.org/10.1016/j.foodhyd.2008.09.017>>. Accessed: Sep. 6, 2021.